ELSEVIER

S0032-3861(96)00492-2

*Polymer* Vol. 38 No. 1, pp. 21–30, 1997

0032-3861/97/$17.00 + 0.00

# The role of dispersed phase morphology on toughening of epoxies

**Julie Y. Qian*†, Raymond A. Pearson*‡§, Victoria L. Dimonie*, Olga L. Shaffer* and Mohamed S. El-Aasser*†§**

**Emulsion Polymers Institute, †Chemical Engineering Department and ‡Materials Science and Engineering Department, Lehigh University, Bethlehem, PA 18015, USA*

*(Received 5 December 1995; revised 12 April 1996)*

The use of structural core/shell latex particles as toughening agents provides a model system which allows independent control of several key factors that influence the fracture toughness of modified plastics. This paper focuses on varying the shell composition of poly(butadiene-*co*-styrene) [P(B-S)] core/poly(methyl methacrylate) (PPMA) shell particles by incorporating acrylonitrile (AN) comonomer into the PMMA shell at various AN/MMA ratios and by crosslinking of the shell at various AN/MMA ratios. It was found that the degree of particle dispersability in the epoxy matrix can be precisely controlled by the AN content in the PMMA shell and by crosslinking the PMMA in the shell. It was also found that the degree of particle dispersability plays a crucial role on the fracture toughness of the modified epoxies. A microclustered morphology provides a much higher toughness than a uniform particle distribution. Copyright © 1996 Elsevier Science Ltd.

**(Keywords: structured latex particles; core/shell particles; toughening plastics)**

## INTRODUCTION

The role of rubber/matrix interface on the fracture toughness of modified plastics has been a controversial issue. The rubber/matrix interface can be varied in terms of interfacial bonding force, thickness, flexibility and composition. However, it is difficult to assess exactly how these changes in the rubber/matrix interface will effect the toughening mechanisms. The main toughening mechanisms operating in a rubber-toughened epoxy are internal cavitation of rubber particles and shear yielding in the matrix, which is believed to be promoted by the cavitation of the rubber particles[1–5]. Obviously, this internal cavitation of rubber particles would require a minimum amount of interfacial adhesion between rubber particles and epoxy matrix. It was believed that the chemical bonding between rubber particles and epoxy matrix is essential to the toughening of epoxies for a carboxyl terminated butadiene acrylonitrile (CTBN)-toughened epoxy system[1,6]. However, a recent study by Huang *et al.*[7] found that interfacial bonding between rubber and epoxy matrix was not important. In their study, the rubber/epoxy interfacial bonding was varied by controlling the number of carboxyl terminated groups in a CTBN rubber. They found that there was a competition between internal cavitation of rubber particles and debonding of the rubber particles from epoxy matrix. When the interfacial adhesion was sufficient, the rubber particles cavitated internally during the fracture; when the interfacial bonding was poor, the rubber particles debonded interfacially from the matrix. However, the fracture toughness of the modified epoxies in these two cases were nearly identical. The same results were found in other rubber-toughened plastic systems, such as nylons[8] and polycyanate[9].

Chen and Jan[10] studied the effect of thickness and flexibility of rubber/epoxy interface on the fracture toughness by end-capping of CTBN rubber with rigid and flexible epoxy end-groups, respectively. They found that the fracture energy of the modified epoxy was dramatically increased up to 2.4 times when the system contained a wider and more flexible interface. Further investigation on the underlying mechanisms have shown that the degree of the internal cavitation of the rubber particles significantly increased as the rubber/epoxy interfacial zone changed from rigid and narrow to flexible and wide. The explanation for this phenomenon was that the size and deformability of the interfacial zone directly affected the triaxial tension around the rubber particles which induced the cavitation of the rubber particles.

An important feature of using core/shell particles as toughening agents for epoxies is the role of the particle/epoxy interface. Compared to conventional CTBN-toughened system, in which rubber particles are directly surrounded by epoxy matrix, a discrete interface is introduced between the particles and the epoxy matrix by the shell polymer of core/shell particles. The architecture of this interface can be well-controlled by varying the shell compositions and the thickness of core/shell particles by emulsion polymerization techniques, so that the role of particle/epoxy interface on toughening of epoxies can be investigated systematically, maintaining the rubbery core unchanged. The effect of shell composition of core/shell particles on toughening of epoxies has been studied by several

§ To whom correspondence should be addressed

investigators. However, the results are conflicting. Sue and co-workers[11] found that introducing glycidyl methacrylate (GMA) into the shell of core/shell particles, which provided chemical bonds at the particle/epoxy interface, had no influence on the toughening; while incorporating AN into the shell improved the dispersability of particles in the epoxy matrix, and increases fracture toughness of the modified epoxies. While Henton *et al.*[12] concluded that the covalent bonding introduced at the rubber/epoxy interface was very crucial to the toughening. In our previous paper[13], we have shown that incorporating both AN and GMA did not improve the toughness of the modified epoxies. Also, it was found that incorporating AN into the shell polymer significantly affected the degree of particle dispersability which directly influenced the final toughness of the epoxies.

This work further investigates the effect of rubber/matrix interface on the toughening of epoxies by systematically varying the amount of AN in the PMMA shell of the core/shell particles and by crosslinking of the shell at different AN contents in the PMMA shell. Therefore, the rubber-matrix interface was systematically varied in terms of physical interaction, extent of interaction and rigidity of the interface. The degree of particle dispersability in the epoxy matrix was characterized using scanning electron microscopy (SEM) and the corresponding toughening mechanism was examined using atomic force microscopy (AFM). The results indicate that the degree of particle dispersability plays a crucial role on the toughening of epoxy. A microclustered morphology provides a much higher toughness than a uniform morphology. The toughening mechanisms in these systems were found to be the internal cavitation of the rubber phase and shear yielding of the epoxy matrix.

## EXPERIMENTAL

### *Materials*

The materials used in preparation of P(B-S) core/PMMA-based shell particles, including monomers, surfactant and initiators, were listed in the previous paper[13]. A brief description of the synthesis of these core-shell latex particles is given below. The epoxy matrix consisted of diglycidyl ether of bisphenol-A epoxy resin (DER® 331, Dow Chemical Co.). The epoxy resin was cured with piperidine (Fischer) to produce a lightly crosslinked polymer.

### *Preparation and characterization of core/shell latex particles*

Uniform P(B-S) core/PMMA-based shell particles were prepared by a seeded emulsion polymerization in a semi-continuous process. The uniformity of the core/shell morphology of the particles was examined using a transmission electron microscope (TEM).

The glass transition temperatures ($T_g$) of the core/shell particles with various shell composition were measured using both differential scanning calorimetry (d.s.c.) and dynamic mechanical spectroscopy (DMS). The samples for d.s.c. measurement were prepared as follow: The core/shell latex particles were cleaned with DDI water for two weeks using a serum replacement and freeze-dried. The d.s.c. traces were recorded in a Mettler TA 3000 at a heating rate of $10^{\circ}C\,min^{-1}$ in a temperature range of $-130$ to $150^{\circ}C$. For the DMS analysis, films of the dried core/shell particles were formed in a compression mould under a force of 1.8 kN and at a temperature of $140^{\circ}C$ for 25 min. The dimension of the film was $60 \times 10\,mm \times 1\,mm$. The dynamic mechanical properties of the films were measured with a Rheometrics RDA-II at a frequency of $7.6\,rad\,s^{-1}$ and a heating rate of $3^{\circ}C\,min^{-1}$, over the same temperature range as for d.s.c. measurements.

### *Preparation and mechanical evaluation of rubber-modified epoxies*

The synthesized P(B-S) core/PMMA shell latex particles were freeze-dried to ensure that the particles did not segregate during the drying process. Then the dried core/shell particles were dispersed into the epoxy using a mechanical stirrer. The detailed procedures and conditions were described in a previous paper[13].

The fracture toughness of the modified epoxies was measured according to the ASTM D5045-91 protocol. The critical stress intensity factor $K_{IC}$ was determined using a single-edge-notched type specimen ($6.4\,mm \times 12.7\,mm \times 80\,mm$) in a three-point bending geometry (SEN-3PB). The tests were performed using an Instron 1011 test machine equipped with a 100 lb load cell. The crosshead rate was $1\,mm\,min^{-1}$. The measurements were repeated on a minimum of five specimens to ensure accuracy. Tensile properties were measured according to the ASTM D638 guideline.

### *Fractography*

The degree of particle dispersability in the epoxy matrix and toughening mechanisms were characterized by SEM and AFM of the fracture surfaces of SEN-3PB specimens. Three different deformation regions which were formed under different deformation conditions in the SEN-3PB test were examined. They are pre-crack region, slow crack growth region (stress-whitened-zone), and fast crack growth region, as schematically represented in *Figure 1*. The matrix and the rubber particles are deformed the most in the slow crack-growth region and less deformed in the pre-crack and fast crack-growth regions.

The SEM examinations were performed in a Joel 6300 scanning electron microscope at an accelerating voltage of 5 kV. Samples were coated with a thin layer of gold–palladium to reduce any charge build-up on the surfaces. The thicknesses of the Au–Pd coatings were approximately around 0.5 nm.

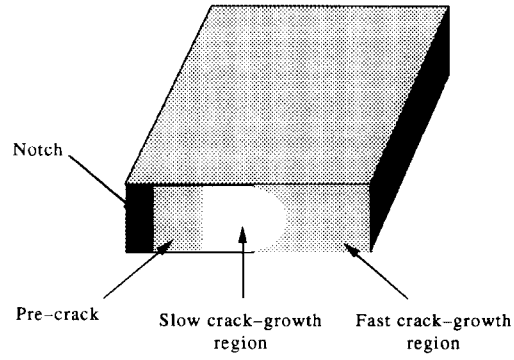


**Figure 1** Schematic representation of three different deformation regions formed in a SEN-3PB test

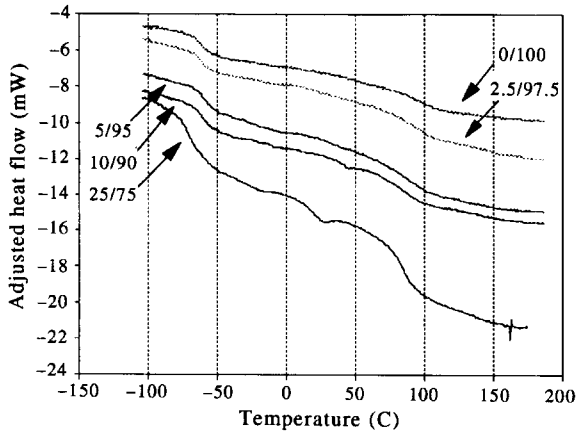


**Figure 2** D.s.c. scans of 50/50 by wt P(B-S) core/PMMA shell particles with various AN content in the PMMA shells (in the range of 0–25% by wt)

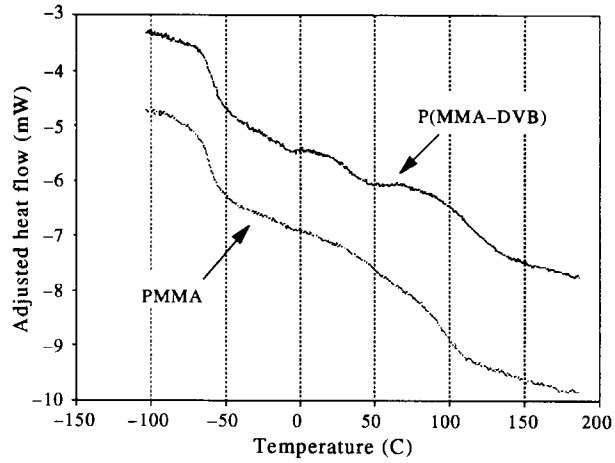


**Figure 4** D.s.c. scans of 50/50 P(B-S) core/PMMA shell particles with 5% by wt DVB in shell and without the crosslinked shell

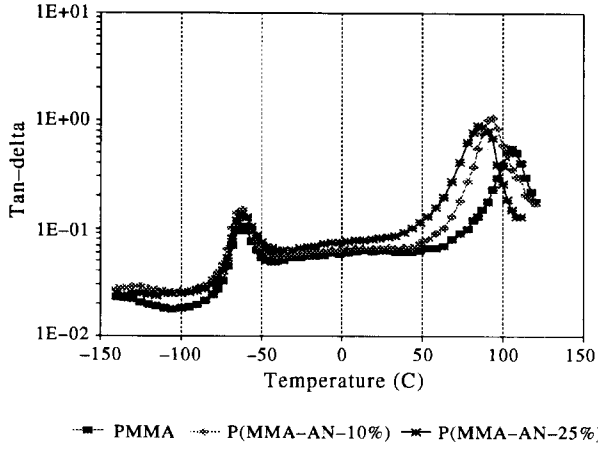


**Figure 3** DMS of 50/50 by wt P(B-S) core/PMMA shell particles with various AN content in PMMA shells: tan $\delta$ as a function temperature

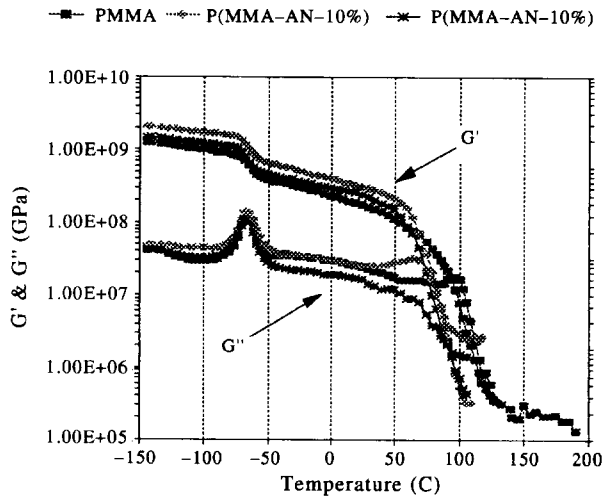


**Figure 5** DMA of 50/50 by wt P(B-S) core/PMMA shell particles with various AN content in PMMA shells: $G'$ and $G''$ as a function of temperature

The AFM examinations were performed using a Park Autoprobe CP AFM of optical deflection type in a contact (repulsive) mode, in which the tip was always touching the surfaces when the feedback loop was on. No further sample treatment was needed. The line profiles of the fracture surfaces were generated on the scanned images to measure the diameter and the height of the cavities.

## RESULTS AND DISCUSSION

### $T_g$ *and modulus of core/shell particles*

The glass transition temperature ($T_g$) and the shear moduli of the synthetic core/shell particles were examined using differential scanning calorimetry (d.s.c.) and dynamic mechanical spectroscopy (DMS). The d.s.c. scans of the P(B-S) core/PMMA-based shell particles with various AN/MMA ratios in the shells are shown in *Figure 2*. The core/shell particles exhibit two $T_g$s. The first $T_g$ located around −65°C corresponds to the $T_g$ of the P(B-S) copolymer cores, and the second $T_g$ located around 95°C corresponds to the $T_g$ of the P(MMA-AN) copolymer shells. The $T_g$s of the P(B-S) cores remained nearly unchanged, while the $T_g$s of the P(MMA-AN) shells decreased with the increase of the AN content in the PMMA shells, which agreed with the compositions of the P(MMA-AN) copolymers[14,15]. This result was confirmed by the dynamic mechanical analysis of the films formed from the corresponding core/shell particles, as shown in *Figure 3*, where the $T_g$s are indicated by tan $\delta$ (i.e. $G'/G''$). These results suggest that a proper amount of AN comonomer had been incorporated into PMMA shell without influencing the composition of P(B-S) cores. The d.s.c. scans of the P(B-S) core/PMMA shell particles with and without a crosslinked shell are displayed in *Figure 4*. Crosslinking the shell simply increased the $T_g$ of the PMMA shell, but did not affect the $T_g$ of the P(B-S) cores.

The storage moduli ($G'$) and loss moduli ($G''$) of P(B-S) core/PMMA shell particles with various AN/MMA ratios as a function of the temperature are shown in *Figure 5*. The P(MMA-AN) shell copolymers exhibit a stronger glass transition drop in $G'$ than expected from the overall ratios of core/shell materials, and P(B-S) seed copolymers yield a corresponding weaker transition. The strong drop in $G'$ suggests the formation of a continuous rigid phase [i.e. P(MMA-AN)] with soft inclusions [i.e. P(B-S)][16–18], which only can be formed by the coalescence of particles with full coverage of the shell

**Table 1** Effect of AN/MMA ratios in PMMA shell of P(B-S) core/PMMA shell latex particles on the mechanical behaviour of the modified epoxies

| AN/MMA wt ratio | $K_{IC}$ (MPa m$^{1/2}$) | $E$ (GPa) | $\sigma_y$ (MPa) |
|---|---|---|---|
| 0/100 | 2.69 ± 0.02 | 2.7 | 64.7 |
| 2.5/97.5 | 2.57 ± 0.05 | 2.7 | 64.4 |
| 5/95 | 2.67 ± 0.05 | 2.5 | 61.2 |
| 7.5/92.5 | 2.57 ± 0.07 | 2.7 | 64.5 |
| 10/90 | 2.57 ± 0.02 | 2.9 | 66.1 |
| 15/75 | 2.20 ± 0.06 | 2.8 | 69.3 |
| 25/75 | 2.21 ± 0.05 | 2.8 | 66.1 |

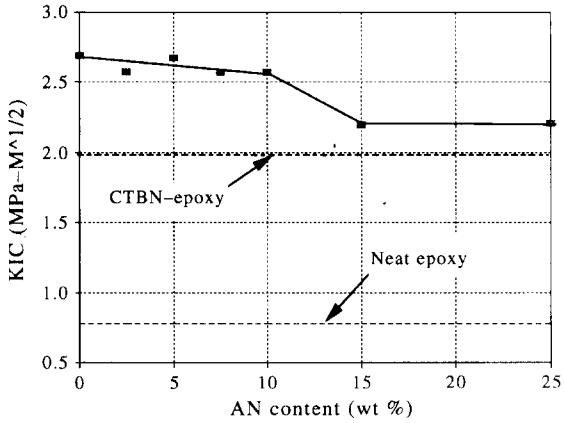


**Figure 6** The effect of AN content in PMMA shell in P(B-S) core/PMMA shell latex particles on the fracture toughness ($K_{IC}$) of the modified epoxies

material onto the core materials. The loss modulus ($G''$) peak for P(B-S), which can be used as indicator for stiffness of the core materials[16], remain unchanged for various AN/MMA ratios, indicating that variation in the shell composition does not interfere with the properties of P(B-S) cores.

*Mechanical behaviour of modified epoxies*

The shell compositions of P(B-S) core/PMMA based shell particles were systematically varied by incorporating AN at various AN/MMA ratios and by crosslinking of the shell at various AN/MMA ratios. AN was expected to increase physical interaction between the particles and the epoxy matrix due to its higher polarity[15,19]. Crosslinking of the shell has several effects: (1) increase the number of chemical bonds within the shell polymers; (2) reduce chain mobility of the shell molecules; (3) increase rigidity of the rubber/epoxy interface.

*Effect of AN/MMA ratio. Table 1* and *Figure 6* display the effect of AN/MMA ratios in the PMMA shell on the mechanical behaviour of the toughened epoxies. Incorporation of AN into PMMA shell did not increase the $K_{IC}$ values. The $K_{IC}$ values of the epoxies slightly decreased with the increase of AN content up to 10%, and dropped off significantly between 10 and 15% AN content, then remained unchanged with a further increase in the AN content up to 25%. The fracture toughness of the epoxies exhibited a transition point between 10 and 15% AN content in the PMMA shell, and the decreases in $K_{IC}$ values at the transition point were around 0.5 MPa m$^{1/2}$.

**Table 2** Effect of crosslinking of shell of P(B-S) core/PMMA shell latex particles on mechanical behaviour of the modified epoxies

| AN/MMA wt ratio | Crosslinking of shell | $K_{IC}$ (MPa m$^{1/2}$) | $E$ (GPa) | $\sigma_y$ (MPa) |
|---|---|---|---|---|
| 0/100 | No | 2.69 ± 0.02 | 2.7 | 64.7 |
| | Yes | 2.49 ± 0.04 | 2.7 | 68.1 |
| 10/90 | No | 2.57 ± 0.02 | 2.8 | 66.1 |
| | Yes | 2.30 ± 0.07 | 2.9 | 66.8 |
| 25/75 | No | 2.21 ± 0.05 | 2.8 | 66.1 |
| | Yes | 2.13 ± 0.04 | 2.9 | 70.1 |

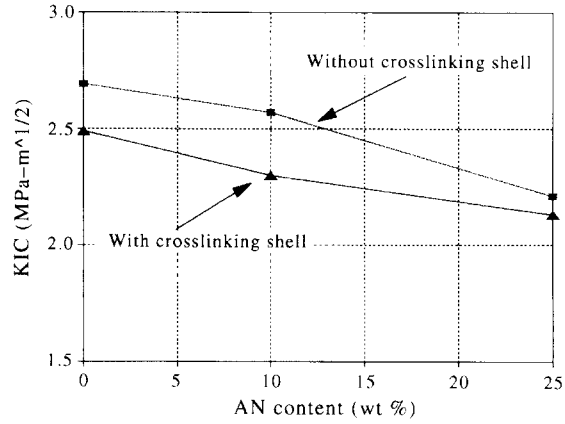


**Figure 7** The effect of crosslinking of the shell on the fracture toughness of the modified epoxies

The decrease in fracture toughness with AN content in the shell polymer was not expected. It has been reported that, for the CTBN-toughened epoxy system, the role of AN is to adjust the solubility of the liquid-rubber[20–23] which controls the miscibility between the liquid rubber and epoxies. The final size of the rubber domains is directly determined by the rubber/epoxy miscibility and an optimum AN content exists for the fracture toughness of CTBN-modified epoxies. For a core/shell particle-modified epoxy system, it was also found that introducing AN into the shell of core/shell particles improved the dispersability of the particles in epoxy matrix and led to a decrease in fracture toughness of modified epoxies.

*Effect of crosslinking of shell.* The effects of crosslinking of the shell on the mechanical behaviour of the modified epoxies are illustrated in *Table 2* and *Figure 7*. Crosslinking of the shell reduced the fracture toughness of the modified epoxies for all the AN/MMA ratios. In the case of particles containing a lower AN content (0 and 5%), the $K_{IC}$ values dropped about 0.2 MPa m$^{1/2}$, while in the case of the particles having a higher AN content (25%), the $K_{IC}$ value was decreased only about 0.1 MPa m$^{1/2}$. Therefore, the effect of AN content on the fracture toughness of blends containing particles with crosslinked shell was minimal.

*Degree of particle dispersability in epoxy matrix*

*Effect of AN/NMA ratio.* The effect of the AN/MMA ratio on the degree of dispersability of the particles in the epoxy matrix is significant. *Figure 8* shows the scanning electron micrographs of the fracture surface of epoxies toughened with core/shell particles with various AN/MMA ratios in the shells. An increase of AN content

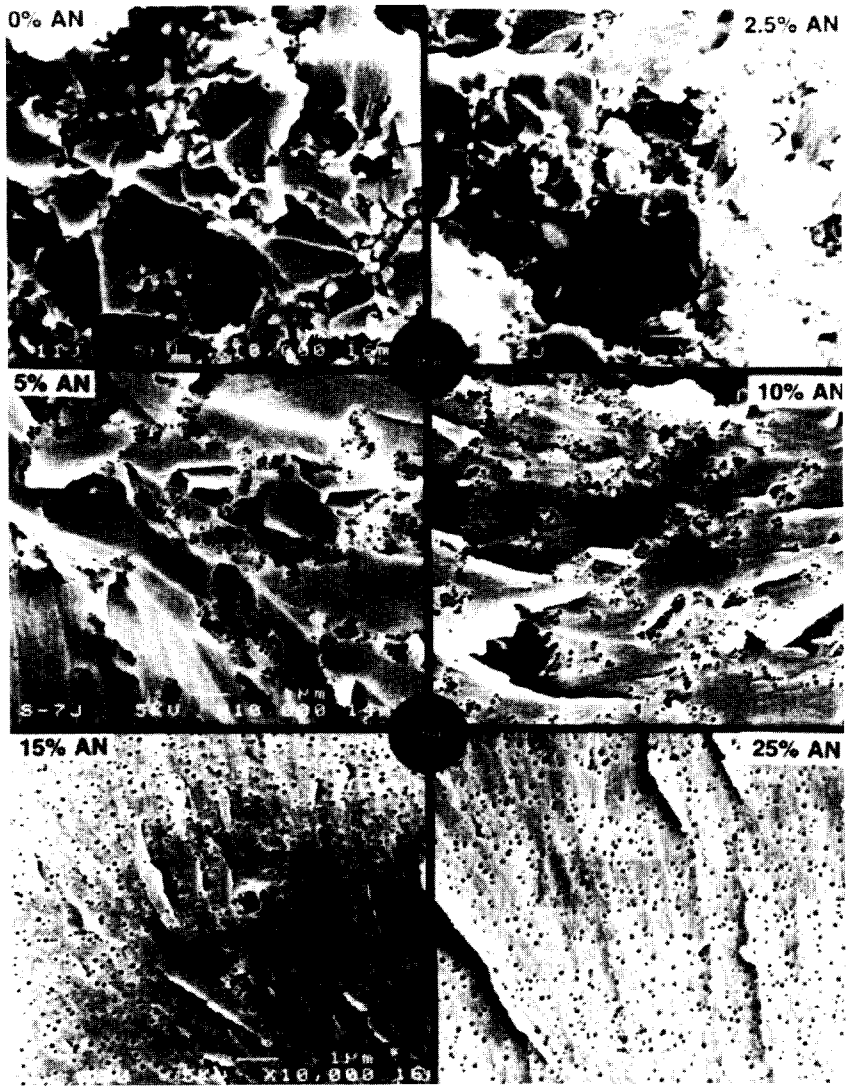


**Figure 8** Scanning electron micrographs of the fracture surfaces of the epoxies toughened with P(B-S) core/PMMA-based shell particles with various AN/MMA ratios in the shells

in PMMA shell improved the degree of dispersability of particles in the epoxies. At lower AN concentrations (10% or less), micro-segregation of the particles was observed, as shown from *Figure 8*; while at high AN concentrations (15% or more), a uniform distribution of rubber particles was achieved, as illustrated in *Figure 8*. Furthermore, for the cases where the microclusters were formed, the size of these clusters decreased approximately from 5 to 1 $\mu$m, as the AN content increased from 0 to 10%. Transition point from micro-segregation morphology to a uniform distribution was found to be between 10 and 15% AN content. This series of experiments clearly demonstrated that the function of the AN in the PMMA shell is to increase the degree of dispersability of the core/shell particle in the epoxy matrix.

It was expected that the improvement of dispersability would increase the fracture toughness[11]. Surprisingly, the results in this work showed an adverse effect, as listed in *Table 1*. The morphology with largest microclusters showed the highest toughness (low AN content in the shell); while those with very uniform particle dispersion show the lowest toughness (high AN content). Moreover, the transition from a micro-segregated to a uniform dispersion corresponds to that of a significant drop in the fracture toughness of the epoxies. This clearly demonstrated the importance of the degree of dispersability of the particles in the epoxy matrix on the toughening of the epoxies. The micro-segregation of particles in the epoxy matrix appears to be desirable to achieve higher fracture toughness.

*Effect of crosslinking of shell. Figure 9* shows the scanning electron micrographs of the fracture surfaces of the epoxies toughened with the core/shell particles with and without crosslinked shells at various AN/MMA ratios. The degree of particles dispersability in the epoxy matrix was increased by crosslinking of the shell, especially in the case of particles containing 10% AN content in the shell, where the crosslinking of the shell resulted in a much more uniform dispersion in the matrix, as illustrated in *Figure 9*. This effect on the particle dispersed morphology by crosslinking of the shell can be attributed to the rigidity of the shell.

Two factors were varied simultaneously by crosslinking of the shells, i.e. degree of the particle dispersability in the epoxy matrix and interfacial structure between the rubber particles and epoxy matrix. In the cases of particles containing a lower AN content in the shell (0 and 10%),

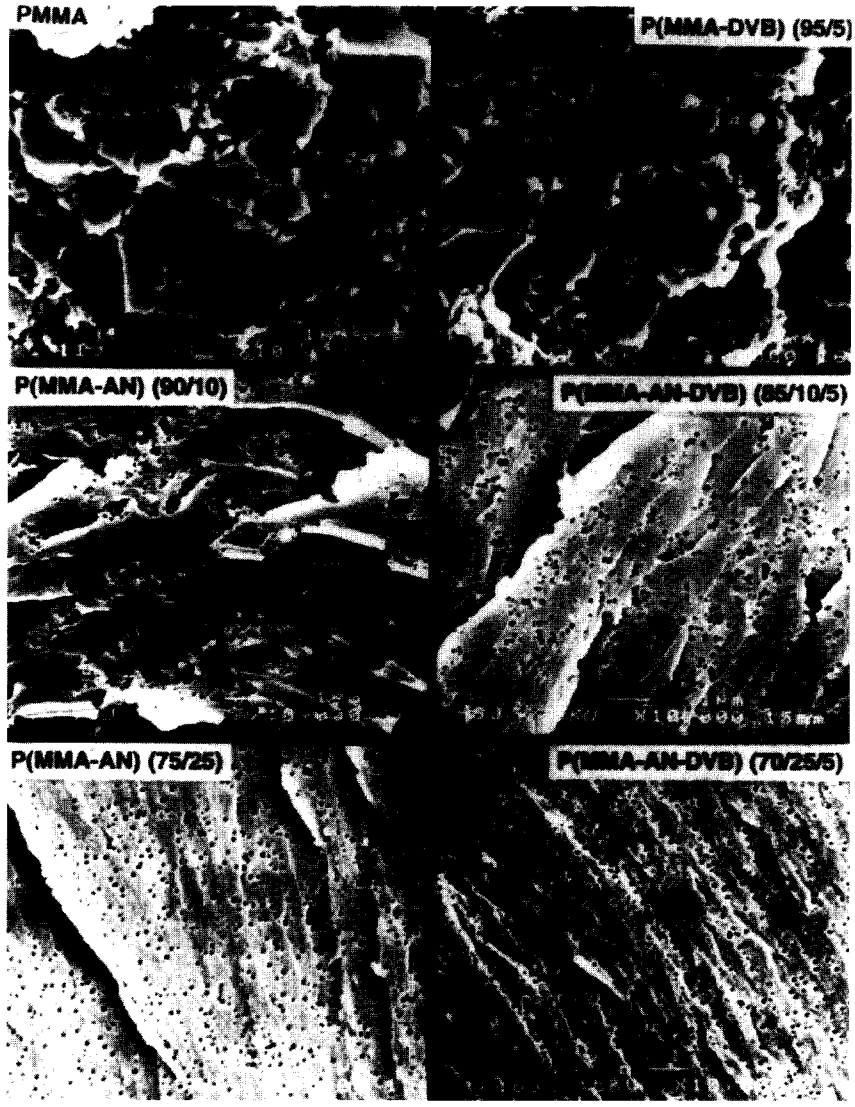


**Figure 9** Scanning electron micrographs of the fracture surfaces of the epoxies toughened with P(B-S) core/PMMA shell particles with and without crosslinked shells

crosslinking of the shell significantly increased the degree of particle dispersability, and resulted in lower fracture toughness, as shown in *Table 2*. This is believed to be mainly due to particle dispersability factor, i.e. blend morphology. In the case of the particles containing a higher AN content (25%) where particles were uniformly distributed in the epoxy matrix, crosslinking of the shell also slightly reduced the fracture toughness. This suggests that besides the dispersion morphology, the final fracture toughness of the epoxies may be weakly dependent upon the structure of the rubber/epoxy interfacial zone. Crosslinking of the shell suppressed the interdiffusion and entanglement of the polymer chains between the shell materials and the epoxies and increased the rigidity of the shell, and as a result, modestly decreased the fracture toughness of the epoxies.

*Deformation mechanism*

*SEM examination.* It is quite noticeable in *Figures 8* and *9* that there are significant differences in the level of roughness at the fracture surfaces of the epoxies. In the cases where the particles were severely segregated, a more rough 'valley-like' pattern was observed, indicating the epoxy matrix was deformed more severely; while in the cases where the particles were less segregated or uniformly distributed in the epoxy matrix, a more smooth 'river-like' pattern was found, indicating the epoxy matrix was less deformed. Furthermore, the roughness of the fracture surface was increased with the decrease of the degree of the particle dispersability in the epoxy. Higher roughness of the fracture surfaces corresponded to a higher fracture toughness of the epoxies. This observation supports the toughening mechanisms which have been proposed by many investigators[1–5] that the main toughening mechanism which consumes the most energy is shear yielding of the matrix.

*AFM examination.* Atomic force microscopy has several advantages over SEM and TEM: (1) high sensitivity in the *Z*-direction, which can be used to provide accurate height information; (2) ability to differentiate materials by their frictional imaging. AFM was used to provide information on the cavitation and subsequent dilation of the matrix.

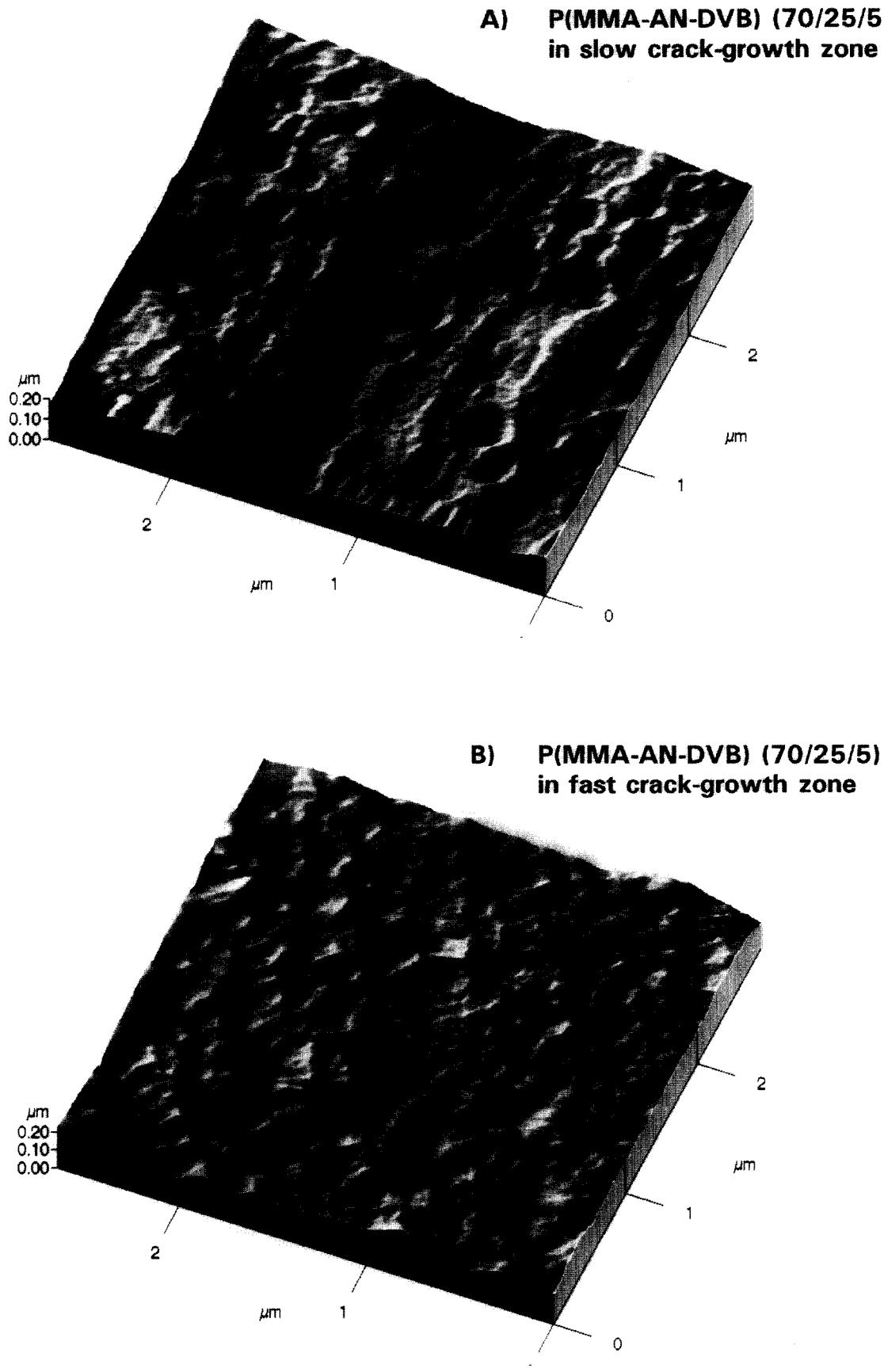


**Figure 10** Atomic force micrographs of the fracture surface of the epoxies modified with P(B-S) core/P(MMA-AN) (75/25) shell particles without crosslinked shells: (A) in slow crack-growth region; (B) in fast crack-growth region

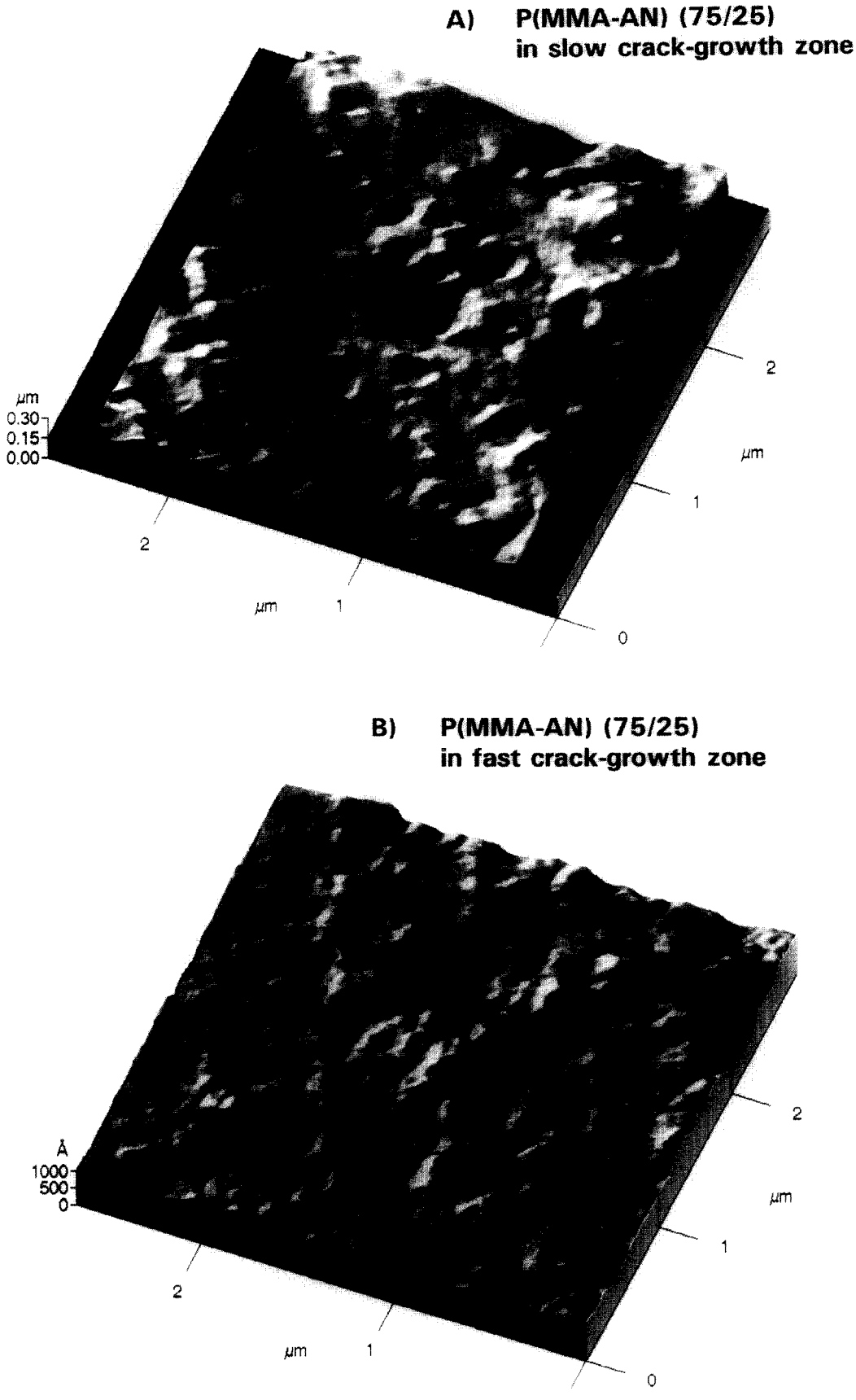


**Figure 11** Atomic force micrographs of the fracture surface of the epoxies modified with P(B-S) core/P(MMA-AN) (75/25) shell particles with crosslinked shells: (A) in slow crack-growth region; (B) in fast crack-growth region

**Table 3** Cavitation of rubber particles in two different deformation regions in modified epoxy

| Shell composition | Particle size (nm)[a] | | Cavity size (nm) | | |
|---|---|---|---|---|---|
| | $D_C$[b] | $D_{C/S}$[b] | $D_S$[c] | $D_F$[c] | Cavitation[d] (%) |
| P(MMA-AN) (75/25) | 84.3 | 100.7 | 199 | 154 | 136 |
| P(MMA-AN-DVB) (70/25/5) | 84.3 | 100.7 | 217 | 174 | 157 |

[a] Measured by TEM
[b] $D_C$ = core size; $D_{C/S}$ = core/shell particle size
[c] $D_S$ = cavity size in the slow crack-growth region; $D_F$ = cavity size in fast crack growth region
[d] Degree of matrix dilation was calculated using the following equation: $(D_S - D_C)D_C \times 100\%$

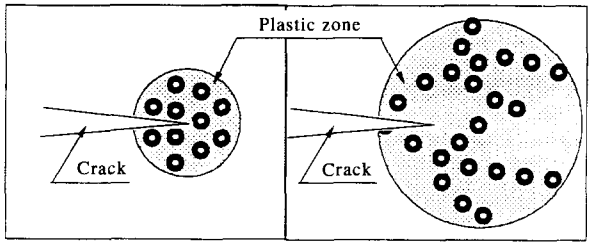


(a) Uniform particle dispersed morphology (b) Micro-clustering morphology

**Figure 12** Schematic diagram of the plastic zone in the modified epoxy with (a) a uniform particle dispersed morphology and (b) a micro-clustering morphology

Two different fracture regions were examined: the slow crack-growth region and fast crack-growth region. The most intense deformation of the particles and the epoxy matrix occurred in the slow crack-growth region. The particles and epoxy matrix were less deformed in the fast crack-growth region. Epoxy systems in which the particles were uniformly distributed in the epoxy matrix were chosen to be studied in order to avoid the complexity caused by the clustering of the particles and roughness of the epoxy fracture surface, i.e. the cases of the epoxies toughened with the core/shell particles containing highest AN content in PMMA shell (25%).

*Figures 10* and *11* present the atomic force micrographs of the fracture surfaces of these epoxies modified with the particles without and with crosslinking of the shells, respectively. The rubber particles were internally cavitated in all the cases. The sizes of the cavitation of the rubber particles were measured from the line profiles, and results are listed in *Table 3*. The cavity diameters were in the range of 200–220 nm in the deformation zone, and so the degree of the matrix dilation exceeded as high as 150%. Comparison of the cavity sizes between the two different fracture regions reveals that the sizes of the cavities in the whitened zones (slow crack-growth zones) were much larger than that in the fast fracture zones. This indicates that the dilation of the matrix is directly influenced by the cracking speed. It should be noted that the cavitation of the rubber particles is necessary to initiate the shear yielding of the epoxy matrix and subsequent plastic dilation.

*Mechanical rationale*

So far, we have demonstrated that micro-segregation of particles in the epoxy matrix provided a higher fracture toughness of the modified epoxy. Similar effects have also been addressed by several investigators who claimed that a co-continuous structure or an inter-connected morphology in a two-phase system resulted in higher fracture toughness. Several mechanical rationales have been proposed to explain this phenomenon. Some investigators attributed this higher fracture toughness to the effect of the particles size[24–29]. In their opinion, the co-continuous morphology simply acts like a larger particle, and therefore, it has a higher bridging efficiency than those of discrete particles. On the other hand, Wu and coworkers[30–34] applied the percolation concept to the rubber-toughened nylon system and predicted that the network morphology was more effective to the toughness than the discrete spherical particles: flocculation to form isolated clusters of the particles was harmful to toughening, while flocculation to form interconnected rubber-particle network was beneficial. Therefore, they concluded that the higher fracture toughness provided by the interconnected rubber-particle network was due to its lower percolation threshold. Yamanaka *et al.*[35] were able to vary the morphology of the CTBN-modified epoxy system from a discrete to an inter-connected morphology by manipulating the rate of phase-separation and the curing. They have shown that the epoxy with a co-continuous structure exhibited an excellent damping efficiency and high peel strength, and predicted that the shear yield resistance of the epoxy might be enhanced by the co-continuous morphology. A schematic diagram explaining the advantages of microsegregation is represented in *Figure 12*.

We propose the following rationale. Cooperative cavitation of the particles in the front of crack tip forms due to the co-continuous clustering morphology of the particles in the epoxy matrix; while in the case of the epoxy with a uniform dispersed morphology, a more random and less coordinated cavitation of the particles is found. The size of the plastic zone in the modified epoxy with a clustered, co-continuous morphology can be much larger than that of the epoxy with a uniform particle dispersed morphology due to the stress field overlapping of adjacent particles, which results in a deeper penetration of the plastic zone into the elastic epoxy matrix. Since the plastic zone can grow much larger when a co-continuous, microclustered morphology occurs, then it is not surprising to observe an increased fracture toughness. Currently, we are designing experiments to examine the effect of 'cell size' on toughness improvements of the co-continuous microclusters.

## CONCLUSIONS

The degree of particle dispersability in the epoxy matrix plays a crucial role in the toughening of the epoxies. Co-continuous micro-segregation of the particles in the epoxy matrix is desirable to achieve the maximum toughness. Incorporating AN into the PMMA shell improves the miscibility between the shell polymer and epoxy matrix, and the degree of particle dispersability in the epoxy matrix can be systematically controlled by varying AN content in the shell. The transition point from a segregated morphology to a uniform distribution is around 10%. Crosslinking of the shell reduces the extent of polymer chain interdiffusion between the shell materials and epoxy matrix, and increases the rigidity of the interfacial zone, and as a result, decreased the particle segregation.

The toughening mechanisms operating in the modified epoxies are internal cavitation of the rubber phase and shear yielding in the epoxy matrix. The superiority in toughness of the modified epoxy caused by the micro-clustered morphology is probably attributed to the cooperative cavitation of the particles in the epoxy matrix which enhances the shear yielding in the epoxy matrix.

## ACKNOWLEDGEMENTS

Financial support for this project from Emulsion Polymers Institute Liaison Program at Lehigh University, NSF-RI Grant No. MSS-9211664, and ACS-PRF Grant No. 25033-G7P is gratefully acknowledged. Discussions with Dr Reza Bagheri on the role of particle dispersion on fracture toughness are gratefully acknowledged.

## REFERENCES

1 Garg, A. C. and Mai, Y. W. *Comp. Sci. Technol.* 1988, **31**, 225
2 Huang, Y., Hunston, D. L., Kinloch, A. J. and Riew, C. K. in 'Toughened Plastics I' (Eds C. K. Riew and A. J. Kinloch), ACS Series 233, 1993, p. 1
3 Pearson, R. A. and Yee, A. F. *J. Mater. Sci.* 1986, **21**, 2475
4 Pearson, R. A. and Yee, A. F. *J. Mater. Sci.* 1989, **24**, 2571
5 Pearson, R. A. and Yee, A. F. *J. Mater. Sci.* 1991, **26**, 3828
6 Kaiser, T. *Chimia* 1990, **44**, 354
7 Huang, Y., Kinloch, A. J., Bertsch, R. J. and Siebert, A. R. in 'Toughened Plastics I' (Eds C. K. Riew and A. J. Kinloch), ACS Series 233, 1993, p. 189
8 Wu, S. *Polymer* 1985, **26**, 1855
9 Yang, P. C., Woo, E. P., Sue, H. J., Bishop, M. T. and Pickelma, D. M. *Polym. Mater. Sci. Eng.* 1990, **63**, 315
10 Chen, T. K. and Jan, Y. H. *Polym. Eng. Sci.* 1991, **31**, 577
11 Sue, H. J., Garcia-Meitin, E. I., Pickelman, D. M. and Yang, P. C. in 'Toughened Plastics I' (Eds C. K. Riew and A. J. Kinloch) ACS Series 233, 1993, p. 259
12 Henton, D. E., Pickelman, D. M., Arends, C. B. and Meyer, V. E. *US Patent* 4,778,851, 1988
13 Qian, J. Y., Pearson, R. A., Dimonie, V. L. and El-Aasser, M. S. *J. Appl. Polym. Sci.* 1995, **58**, 439
14 Peyser, P. in 'Polymer Handbook' (Eds J. Brandrup and E. H. Immergnt), 3rd Edn, John Wiley & Sons, 1990, p. VI/279
15 Coleman, M. M., Graf, J. F. and Painter, P. C. 'Specific Interactions and the Miscibility of Polymer Blends'. Technomic, Lancaster, PA, 1991
16 Sperling, L. H., Chiu, T. W., Hartman, C. P. and Thomas, D. A. *J. Polym. Mater.* 1972, 331.
17 Delgado, J., El-Aasser, M. S., Silebi, C. A. and Vanderhoff, J. W. *J. Polym. Sci., Polym. Chem. Ed.* 1986, **24**, 861
18 Kong, X. Z., Pichot, C., Guillot, J. and Cavaille, J. Y. in 'Polymer Latex, Preparation, Characterization and Applications' (Eds Daniels, E. S., Sudol, E. D. and El-Aasser, M. S.), ACS Symp. Series 492, 1992, p. 163
19 Verchere, D., Sautereau, H., Pascault, J. P., Moschair, S. M., Riccardi, C. C. and Williams, R. J. J. *Polymer* 1989, **30**, 107
20 Sultan, J. N. and McGarry, F. J. *Polym. Eng. Sci.* 1973, **12**, 29
21 Bucknall, C. B. and Yoshii, T. *Br. Polym. J.* 1978, **10**, 53
22 Bucknall, C. B. and Partridge, I. K. *Polym. Eng. Sci.* 1986, **26**, 54
23 Mulhaupt, R. *Chimia* 1990, **44**, 43
24 Mataga, P. A. *Acta Metall* 1989, **37**, 3349
25 Min, B. G., Hodgkin, J. H. and Stachurski, Z. H. *J. Appl. Polym. Sci.* 1993, **50**, 1065
26 Iijima, T., Miura, S., Fukuda, W. and Tomoi, M. *Eur. Polym. J.* 1993, **29**, 1103
27 Murakami, A., Saunders, D., Ooishi, K. and Yoshiki, T. *J. Adhesion* 1992, **39**, 227
28 Yamanaka, K. and Inoue, T. *Polymer* 1989, **30**, 662
29 Cecere, J. A. and McGrath, J. E. *Polym. Prepr.* 1986, **27**, 299
30 Wu, S. *J. Appl. Polym. Sci.* 1988, **35**, 549
31 Wu, S. *Polym. Eng. Sci.* 1990, **30**, 753
32 Hsu, W. Y. and Wu, S. *Polym. Eng. Sci.* 1993, **33**, 293
33 Margolina, A. and Wu, S. *Polymer* 1988, **29**, 2170
34 Wu, S. and Margolina, A. *Polymer* 1990, **31**, 972
35 Yamanaka, K., Takagi, Y. and Inoue, T. *Polymer* 1989, **60**, 1839